5902 *Macromolecules* **2001,** *34,* 5902−5909

Structure Development during Shear Flow Induced Crystallization of i-PP: In Situ Wide-Angle X-ray Diffraction Study

Rajesh H. Somani, Benjamin S. Hsiao,* and Aurora Nogales[†]

Department of Chemistry, State University of New York, Stony Brook, New York 11794-3400

Hitesh Fruitwala, Srivatsan Srinivas, and Andy H. Tsou

ExxonMobil Chemical Company, Baytown Polymers Center, Baytown, Texas 77522

Received April 9, 2001; Revised Manuscript Received June 8, 2001

ABSTRACT: In situ synchrotron wide-angle X-ray diffraction (WAXD) was used to monitor crystallization of isotactic polypropylene (i-PP) in the subcooled melt at 140 °C after step shear. The melt was subjected to a shear strain of 1430% at three different shear rates (10, 57, and 102 s^{-1}) using a parallel-plate shear apparatus. WAXD results were used to determine the type (α- and β-crystals), orientation, and corresponding mass fractions of i-PP crystals. It was found that formation of oriented α-crystals occurred immediately after application of the shear field. Subsequently, growth of primarily unoriented β-crystals was observed. WAXD patterns clearly showed that β-crystals grew only after the formation of oriented α-crystals in the sheared i-PP melt. The contribution of β-crystals to the total crystalline phase was as high as 65−70% at high shear rates (57 and 102 s^{-1}) and low (20%) at low shear rates (10 s^{-1}), which was attributed to the different amount of surface area of oriented α-crystal cylindrites generated at different shear rates. The growth of β-crystals which is related to the surface area of the oriented α-form crystalline assembly has been proposed earlier. Also, the unoriented nature and fast growth of the β-crystals determined from WAXD experiments provide an explanation for the 2 orders of magnitude increase in the kinetics of crystallization of the unoriented structures, which was previously observed (but not explained) in our crystallization study by small-angle X-ray scattering (SAXS).

Introduction

Thorough knowledge of flow-induced crystallization in polymer melts is essential to control industrial processing methods such as extrusion, injection, and blow molding and resultant product properties. Many research groups[1−17] have investigated this subject, especially the effect of shear field and its relationship with the morphology. It is widely accepted that the sheared polymer melts exhibit an increased rate of crystallization and a different morphology compared with those of a quiescent melt. The resultant morphology has been shown to have direct impact on the improved properties, which is attributed to the oriented structures developed by the applied flow fields.[18−21] Understanding the influence of the applied shear field (total strain, shear rate, and temperature) on the characteristic features of the crystalline phase, i.e., its quantity and nature (habits and orientation), is therefore paramount to the optimization of processing conditions involving shear.

It has been reported that, of all the crystalline forms of isotactic polypropylene (i-PP), the β-crystals demonstrate different performance characteristics, including improved elongation at break and impact strength.[22] The β-crystals can be obtained by addition of certain heterogeneous nucleating agents by crystallization in a temperature gradient or by shear-induced crystallization. Varga et al.[23] studied shear-induced crystallization of isotactic polypropylene and homo, block, and random copolymers using a thermal optical technique and showed that shearing caused development of α-row-nuclei; i.e., the macromolecules in the melt under shear were stretched and aligned in a form of fibrillar bundles along the flow direction. The preoriented molecules crystallized easily and acted as nucleating sites (self-nuclei) for bulk crystallization. The surface of the in situ formed α-row-nuclei induced epitaxial growth of folded chain lamellae that filled the space normal (perpendicular) to the row nuclei, resulting in a supramolecular structure of cylindrical symmetry. Varga et al.[24] also studied interfacial morphologies and the structure of the crystalline phase in carbon fiber-reinforced i-PP composites. It was observed that the shear-induced supramolecular structure consisted of two crystalline forms: α and β. The α-form triggered the growth of the β-form in i-PP. They speculated that, during shear-induced crystallization of i-PP, the α-row nuclei formed in situ could also induce the growth of the β-form.

Lovinger and co-workers studied the microstructure of melt-grown dendritic aggregates of α- and β-crystals of i-PP by crystallization in a temperature gradient.[25−27] They observed that initially, as the crystallization interface was established and crystallization began, nucleation of new spherulites at any point in the sample took place in the α-crystals almost without exception. Furthermore, they reported that under ordinary crystallization conditions in i-PP β-crystals nucleation was extremely rare, and only α-crystals spherulites were obtained by primary nucleation. However, the i-PP samples crystallized in a temperature gradient resulted in a well-oriented material of high β-crystals content, and they concluded that the β-crystals were initiated by growth transformation (which caused the chains to pack in the β-unit cell rather than the α-unit cell) along the oriented α-front. They also found that the β-crystals grew considerably faster than the α-crystals and that the α- to β-transformation points diverged across the

---

* Author for correspondence. e-mail: bhsiao@notes.cc.sunysb.edu.
[†] Instituto de Estructura de la Materia, Spain.

10.1021/ma0106191 CCC: $20.00

sample and interrupted the growth of oriented α-crystal fibrils. From the in situ polarization photomicrographs, they observed that the transformation of α to β was randomly induced and that it could be initiated at a single point, at a series of points on the melt-solid interface, along the entire length of the interface or—very rarely—by actual primary nucleation.

Several reports in the literature[28−30] support the observation that without shearing the α-modification prevails, whereas the β-crystals appear in sheared samples. For example, Moitzi and Skalicky[29] observed that a notable fraction of the β-crystals appeared in sheared samples of i-PP even at a low shearing rate of 4 s^{-1}. Hubeny and Muschik[30] also observed β-crystals of i-PP form in the sheared melt without nucleating agents. Although it has been widely accepted that the β-crystals form in a sheared i-PP melt, quantitative information on the different crystalline phases (α and β) under various conditions of shear have not been reported in the literature.

The in situ small-angle X-ray scattering (SAXS) technique provides a direct measure of the development of oriented structures, the kinetics, and their fractions.[31,32] In our previous publication,[32] we reported results of SAXS experiments with i-PP at 140 °C under step shear conditions. The SAXS results were used to characterize morphological features and determine oriented/unoriented fractions in the polymer bulk. However, the nature of the constituent crystalline forms (α or β) could not be ascertained from this study. The SAXS data showed that shear affected not only the kinetics of the oriented crystals but also kinetics of the unoriented crystals. (Its rate also increased about 2 orders of magnitude.) The reasons for the increase in the kinetics of the unoriented crystals were not fully understood at that time.

In this paper we report results from in situ WAXD experiments with i-PP under the same conditions of shear as used in our previous SAXS study. The results clearly show that oriented α-crystals of i-PP form immediately after shear. Subsequently, the growth of β-crystals was observed. The contributions of α-crystals and β-crystals to the total crystalline phase were also determined from the WAXD data. Results showed that the shear rate affected the amount of β-crystals. The final contribution of β-crystals to the total crystalline phase was 70% at the shear rate of 102 s^{-1}. The intensity of the (300) reflection, characteristic of the β-crystals, did not show noticeable azimuthal dependence leading to the conclusion that the β-crystals were primarily unoriented. The increase in the crystallization kinetics of unoriented crystals (observed from the previous SAXS study) can therefore be attributed to the growth of the unoriented β-crystals. In all experiments, under different conditions of shear, the oriented α-crystals form first and the β-crystals grow afterward. This suggests that the surface of the oriented α-crystal assembly (in the form of cylindrites) provide nucleation sites for the growth of unoriented β-crystals, which is consistent with the earlier reports.[23−27]

Experimental Section

The step shear experiments followed the short-term shear protocol isolating the effects of flow (rate and strain) on subsequent structure development, as originally demonstrated by Janeschitz-Kriegl and co-workers.[9] This method essentially eliminates consequence of reorientation of crystallites by stopping flow before appreciable crystallization occurs. The details of the sample preparation, experimental setup, and procedure have been given in a recent publication.[32] In the WAXD experiments we used the same i-PP resin (M_w = 368 965) and experimental procedures, including the shear field conditions, as in the SAXS experiments.[32] All samples were subjected to the same thermal history; the samples were heated to 200 °C and held for 5 min to eliminate residual structures, and the polymer melt was then cooled at 30 °C/min to 140 °C (the temperature of experiment). The crystallization half-time at the quiescent state of this sample is about 10 000 s at 140 °C. A high strain value of 1430% was used in all experiments. The duration of the step shear was 1.4, 0.25, and 0.14 s, corresponding to shear rates of 10, 57, and 102 s^{-1}, respectively. The WAXD images (10 s acquisition time) were collected continuously: before, during, and after cessation of the applied shear.

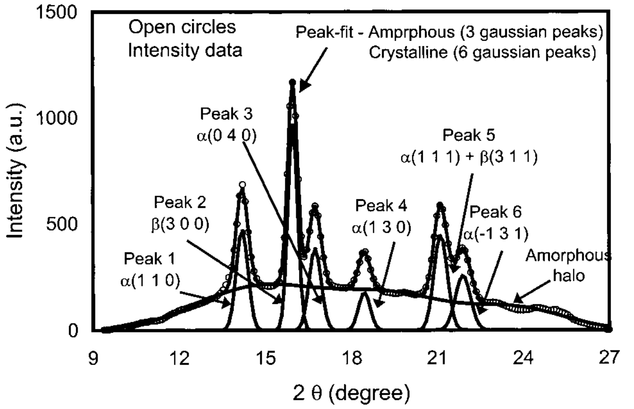

Figure 1. Deconvolution of an example WAXD intensity profile for calculation of the contributions of amorphous and total crystalline phase (and its components, α- and β-crystals) in the polymer melt after shear (profile at $t = 1185$ s, rate = 102 s^{-1}, strain = 1430%, $T = 140$ °C).

Wide-Angle X-ray Diffraction Measurements. WAXD measurements were carried out at the X3A2 synchrotron beamline in the National Synchrotron Light Source (NSLS), Brookhaven National Laboratory (BNL). The wavelength of the synchrotron radiation was 1.54 Å. A 2D MAR CCD X-ray detector (MARUSA) was employed for the detection of 2D WAXD images, having a resolution of 512 × 512 pixels (pixel size = 257.6 μm). The sample-to-detector distance was 140 mm. An air scattering pattern (10 s acquisition time) at a temperature of 140 °C with no sample between the two windows of the shear stage was also collected. The air scattering pattern was used for background correction of the WAXD data; the X-ray data were also normalized for the sample thickness. Subsequent analysis of the X-ray data was carried out using the corrected and normalized WAXD patterns.

WAXD Data Analysis. From the 2D WAXD patterns, the circularly averaged intensity profile was obtained. A typical averaged WAXD profile and the peak-fit procedure used to deconvolute the peaks are shown in Figure 1. In the WAXD profile of the α-crystals of i-PP, the following reflections are usually expected: (110) at $2\theta = 14.1°$, (040) at 16.9°, (130) at 18.5°, (111) at 21.4°, and (−131) at 21.8°.[33] The β-crystals are expected to exhibit the following reflections: (300) at $2\theta = 16.1°$ and (311) at 21.4° (this reflection coincides with the (111) reflection of the α-crystals). Note that the (300) reflection of the β-crystals is the stronger of the two and is distinctly separated from all other α-crystal reflections and thus is usually used as a marker for the β-crystals. From the WAXD profile, the peak position, peak height, peak width, and integrated intensity (peak area) for each crystal reflection and the amorphous background can be extracted (Figure 1). In this study, the deconvolution procedures were carried out using a custom code capable of dealing with time-resolved spectra. The shape of the amorphous contribution was obtained from the image of the isotropic melt before shear. Three Gaussian functions were used to describe the amorphous background.

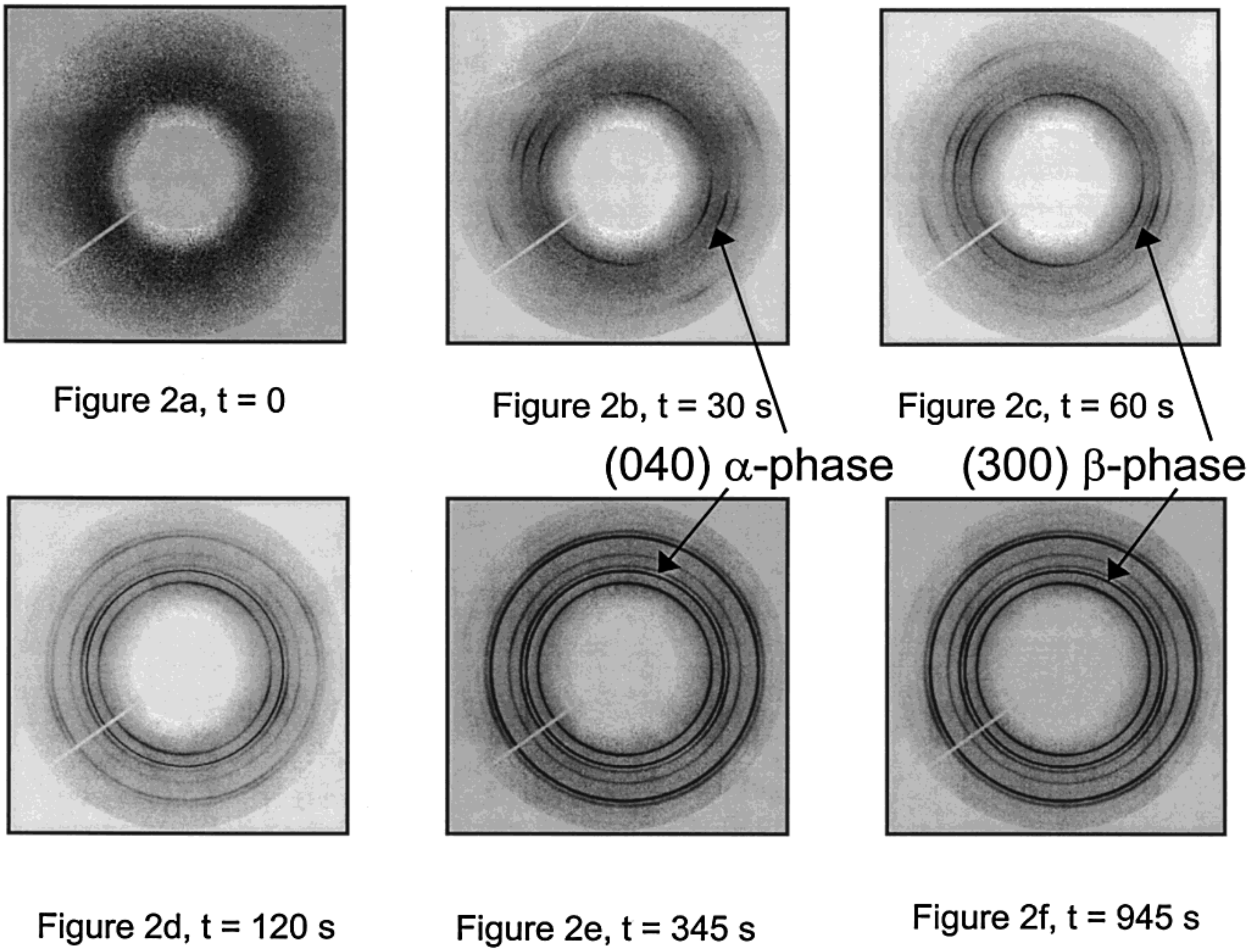

Figure 2a, t = 0

Figure 2b, t = 30 s

Figure 2c, t = 60 s

Figure 2d, t = 120 s

Figure 2e, t = 345 s

Figure 2f, t = 945 s

Figure 2. 2D WAXD patterns of i-PP at 140 °C before and after step shear (shear rate = 102 s^{-1}, strain = 1430%): (a) image of amorphous melt before shear, (b) image showing oriented α-crystal reflections, (c) image first showing reflection of *β*-crystals, (d, e) images showing growth of α- and *β*-crystals, and (f) image after the completion of crystallization.

Additional Gaussian functions were inserted, and an iterative peak-fit procedure was used to fit the crystalline reflections of WAXD profiles. Thus, the peak parameters (height, width, and area) of each crystal reflection were obtained.

The following procedure was adopted to calculate of the total crystalline fraction and contributions from each crystalline phase (α and *β*). From the iterative peak-fit procedure, the percent area of each peak (corresponding to mass fraction of each reflection) and of the amorphous background curve were extracted. The percent amorphous phase in the polymer bulk was calculated from the area percentage of the amorphous background curve. The percent total crystalline phase in the polymer melt was then obtained (100 − % amorphous). The contributions from α- and *β*-crystals in the total crystalline phase was estimated from the ratio of the (100) (for α-form) and (300) (for *β*-crystals) reflection peak areas.

Results

WAXD Patterns after Shear. A representative series of two-dimensional (2D) WAXD patterns of i-PP at 140 °C before and after application of step shear (102 s^{-1} shear rate and 1430% strain) are shown in Figure 2. The selected, circularly averaged one-dimensional (1D) WAXD intensity profiles at various times after shear are shown in Figure 3. The initial pattern ($t = 0$, Figure 2a) shows diffuse scattering without any crystal reflections arising from a completely amorphous polymer melt. This pattern was observed before shear in all experiments, confirming thermal clearing of all residual crystalline structures in the i-PP melt. The corresponding 1D averaged intensity profile at time 0 (Figure 3) is typical of an amorphous polymer melt.

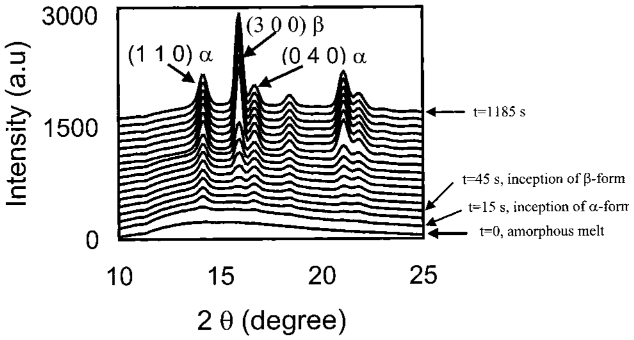

Figure 3. 1D circularly averaged WAXD intensity profiles as a function of scattering angle, 2*θ*, of i-PP melt at various times after shear (shear rate = 102 s^{-1}, strain = 1430%, T = 140 °C); the inception time of α- and *β*-crystals are also shown.

Figure 2b shows the diffraction pattern obtained 30 s after the applied shear. Sharp α-crystal reflections are clearly observed; also, the azimuthal breadths in the intensity of crystal reflections are relatively narrow, indicating that the orientation of the crystals is high. It should be emphasized that the growth of oriented α-crystals was observed immediately after shear. (The first pattern after shear ($t = 15$ s) showed the oriented crystal reflections.) The strongest (110) reflection of α-crystals is clearly seen in the 1D WAXD profile at *t* = 15 s (Figure 3). These WAXD observations are consistent with the SAXS results that discrete meridional maxima from the oriented scatterers were observed immediately after shear.

Figure 2c shows the diffraction pattern at *t* = 60 s after shear; the (300) reflection of β-crystals can be clearly identified in the WAXD pattern. The 1D WAXD profiles in Figure 3 show β-phase actually occurs at *t* = 45. It is noted that the inception of the β-crystals phase (*t* = 45 s) takes place after the inception of the α-crystals phase (*t* = 15 s). The intensity of both α- and β-crystal reflections become stronger with time due to the growth of the crystallites. After a certain time, the intensity of all crystal reflections remained constant, and no significant change was observed in the diffraction pattern, indicative of completion of crystallization, which is consistent with previous SAXS results.

In Figure 2c, the observation of the initial (300) reflection suggests that the first formed β-crystals are oriented; however, the diffraction patterns obtained at *t* = 120, 345, and 945 s after shear (Figure 2d−f) show that the (300) reflection becomes isotropic with no variation in azimuthal intensity, indicating the unoriented nature of the β-crystals. Figure 2d−f also shows that the α-crystal reflections remain oriented, even though the degree of orientation decreases. In addition, the WAXD profiles in Figure 3 show that the average intensity of the (300) reflection becomes much stronger with time compared to the intensities of the reflections from the α-crystals. Interpretations of the WAXD observations and the nature of the orientation of the α- and β-crystals will be discussed later.

Effect of Shear Rate. The variation of the shear parameters including shear rate and strain, obviously, will affect the degree of molecular orientation in the polymer melt, which in turn will influence the nature (habit and orientation) as well as the kinetics of the crystalline phase. The SAXS results have shown that,[32] at a given shear rate and a constant strain, only polymer molecules with chain length above a “critical orientation molecular weight” can remain oriented and form stable shear-induced primary nuclei. The short chain molecules relax in a very short time and cannot easily stay oriented. The oriented crystals originate from these orientation (flow)-induced nuclei and grow by a process of secondary nucleation in a direction perpendicular to the flow. It is evident that all polymer molecules including the relaxed low molecular weight species take part in the crystal growth, but the net crystal orientation will be lost rapidly if the surrounding molecules (of the nuclei) are largely unoriented. The SAXS results[32] have been used to quantify the amount of total oriented crystal fraction in the crystalline phase, and it was observed that the oriented fraction of the crystals is particularly sensitive at low shear rates; however, no significant change in the oriented fraction was observed at the shear rates above 60 s^{-1}.

Figure 4 illustrates the time evolution of the mass fractions of the amorphous and crystal (both α- and β-forms) phases after shear at a rate of 102 s^{-1}. The percentage of the total crystalline phase (the sum of α- and β-crystals) in the polymer melt as a function of time is also shown in Figure 4. The rise in the total crystalline phase vs time is almost instantaneous due to crystallization of the melt immediately after shear. Correspondingly, the decrease in the percent amorphous phase is also observed. Both total crystalline and amorphous phases reach a plateau after a certain time (~300 s), indicating that crystallization is complete. At a shear rate of 102 s^{-1} (and strain of 1430%) the i-PP melt at 140 °C crystallizes in less than 500 s after shear, which is consistent with the observations from SAXS.[32] The α-phase and β-phase growth curves in Figure 4 show that initial contribution to the total crystalline phase is only from the α-crystals (the β-crystals are absent). A short time later, the rise in the β-phase is observed, as shown in the inset in Figure 4. Subsequently, the β-phase contribution to the total crystalline phase increases rapidly, and at the shear rate of 102 s^{-1}, it is significantly more than the α-phase at the end of the crystallization period.

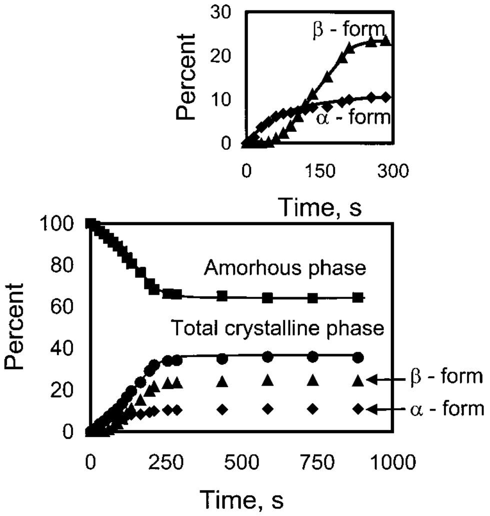

Figure 4. i-PP melt structural development after shear (shear rate = 102 s^{-1}, strain = 1430%, T = 140 °C) and the percent contributions of amorphous and total crystalline phase (and its components, α- and β-form) in the polymer bulk. The inset shows the growth of the α- and β-phases immediately after shear.

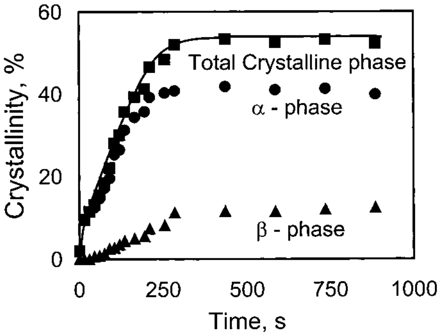

Figure 5. Total crystalline phase development in the i-PP melt at 140 °C after shear (shear rate = 10 s^{-1}, strain = 1430%) and contribution and growth of α- and β-crystals.

It is interesting to note that the contribution of the β-phase to the total crystalline phase decreases substantially at low shear rates. Figure 5 shows the crystal fractions (total, α-, and β-forms) developed (at 140 °C) as a function of time after shear at a shear rate of 10 s^{-1} (strain of 1430%). We note that the total crystallinity (mass fraction) of i-PP polymer is higher at the lower shear rate of 10 s^{-1} compared to that at the higher shear rate of 102 s^{-1}. As before, initially the contribution to the total crystalline phase is mainly from the α-crystals due to the absence of the β-crystals. The β-crystals

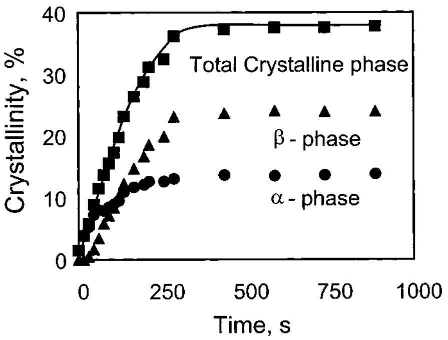

Figure 6. Total crystalline phase development in the i-PP melt at 140 °C after shear (shear rate = 57 s^{-1}, strain = 1430%) and contribution and growth of α- and *β*-crystals.

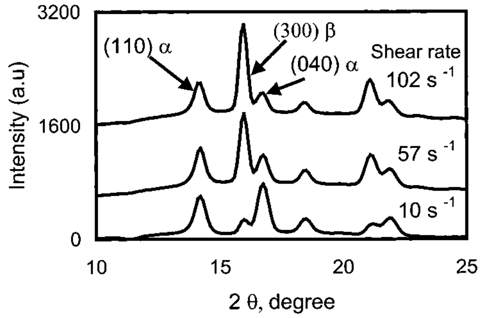

Figure 7. 1D WAXD intensity profiles at $t = 1185$ s after shear (long after the end of crystallization) of i-PP melt at 140 °C at different shear rates (strain = 1430%).

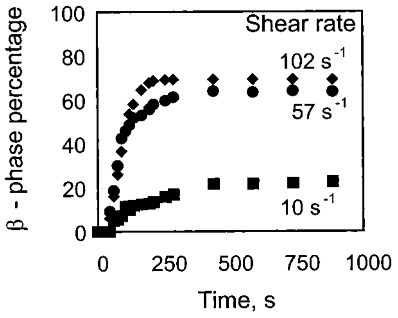

Figure 8. Ratio of the *β*-crystal to the total crystalline phase and its growth in the i-PP melt at 140 °C after shear at different shear rates (strain = 1430%).

growth is developed soon afterward. Although the percent total crystallinity is higher at the lower shear rate (10 s^{-1}), the *β*-crystals contribution to the total crystalline phase is significantly reduced (20%), compared to its contribution (70%) to the total crystalline phase at the higher shear rate (102 s^{-1}). The effect of shear rate is thus quite significant on the growth and the final contribution of the *β*-crystals in the polymer. The corresponding results of the WAXD experiment at a shear rate of 57 s^{-1} are shown in Figure 6. The evolution of the α-, *β*-, and total crystalline phase growth profiles at the shear rate of 57 s^{-1} is very similar to that at a shear rate of 102 s^{-1}. For example, the contribution of the *β*-phase to the total crystalline phase is about 65%, which is very close to the value of 70% at a shear rate of 102 s^{-1}. It appears that the increase in the amount of *β*-phase reaches a plateau value at high shear rates (>57 s^{-1}). The above observation is consistent with the SAXS results where the oriented crystal fraction also reached a plateau above a shear rate of 60 s^{-1}.[32]

To further understand the effect of shear rate on the inception time and the ratio of the *β*-crystals to α-crystals based on the final crystal phase, the WAXD results at all three shear rates (10, 57, and 102 s^{-1}) have been compiled and are shown in Figures 7 and 8. The averaged 1D WAXD intensity profiles at $t = 1185$ s after shear (corresponding to the plateau region on the intensity vs time curve, i.e., at the end of crystallization) at different shear rates are shown in Figure 7. Figure 8 shows the time evolution of the percent contribution of the *β*-crystal growth at various shear rates. The variation in the intensities of the (110) and (040) reflections from the α-crystals and the (300) reflection from the *β*-crystals as a function of the shear rate can be clearly seen in Figure 7. At a shear rate of 10 s^{-1}, both the (110) and (040) reflections (of α-crystals) are stronger than the relatively weak (300) reflection (of *β*-crystals). Thus, the contribution of α-crystals to the total crystalline phase is much higher than that of *β*-crystals at low shear rates. At high shear rates (57 and 102 s^{-1}) the strength of the (300) reflection from the *β*-crystals is stronger than that of the (110) and (040) reflections from the α-crystals. Figure 8 shows that the time of inception and the growth of the *β*-crystals is slightly earlier for the shear rates of 57 and 102 s^{-1} than for the shear rate of 10 s^{-1}. Also, the percent contribution of *β*-crystals is only 20% at the low shear rate (10 s^{-1}), compared to 65−70% at high shear rates (57 and 102 s^{-1}). Figures 7 and 8 show that the difference in the contribution to the total crystalline phase from the *β*-crystals at the different shear rates is substantial; however, the difference is not significant between the shear rates of 57 and 102 s^{-1}. These results clearly show that both the inception time and the amount of *β*-crystals are shear rate dependent. The SAXS results[32] have shown that the oriented crystal fraction in the final polymer bulk is directly related to the applied shear rate. (It is very sensitive at low shear rates, but it reaches a plateau at shear rates above 60 s^{-1}.) The WAXD results in Figures 7 and 8 show a very similar trend for the amount of *β*-phase formed by shear. The results suggest that there is a direct link between the oriented α-crystals and the growth and amount of the *β*-crystals. They are consistent with the assertion that the surface of the oriented α-crystal assembly (in the form of cylindrites) provides nucleation sites for the growth of *β*-crystals, which has been proposed earlier.[23−27] At low shear rates, as lower amounts of the oriented α-crystals are formed, the quantity of the induced *β*-crystals are low as expected.

Crystallization Kinetics. In a previous publication,[32] the results of the kinetics of crystallization (half-time of crystallization) for both oriented and unoriented components of i-PP at 140 °C under different shear rates have been reported. Here, the half-time of crystallization for the *β*-crystalline phase as a function of shear rate was determined from the *β*-crystal growth profiles (Figures 8) at different shear rates. The half-time of crystallization was taken as the time at which the relative crystallinity of the *β*-crystals phase reached a value of 0.5. The results are shown in Figure 9. About 2 orders of magnitude increase in the kinetics of crystallization of the *β*-crystalline phase can be clearly seen in Figure 9.

Figure 9 also shows the half-time of crystallization of the unoriented crystals at different shear rates, which were calculated from the results of previously reported SAXS experiments.[31] The half-time of crystallization of the unoriented crystals were calculated from the cor-

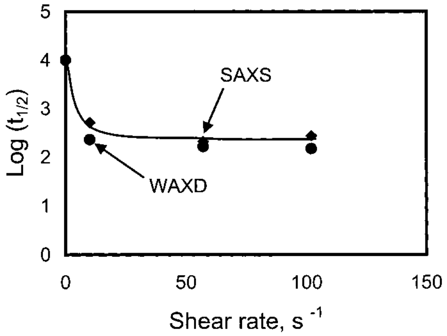

Figure 9. Half-time of crystallization of the β-crystals (WAXD) and the unoriented crystals (SAXS) at different shear rates (strain = 1430%, T = 140 °C).

responding time evolution SAXS integrated intensity profiles at different shear rates. The half-time of crystallization was taken as the time corresponding to an unoriented fraction = 0.5. The calculated values of the half-time at different shear rates of the β-crystals (WAXD) and of the unoriented crystals (SAXS) show a good agreement within the experimental error. These observations indicate a direct relationship between the unoriented crystals and the β-phase. This will be discussed in detail in the next section.

Discussion

In this section, interpretation of the WAXD results and the brief conclusions from the previously reported SAXS results are organized to highlight our interesting findings. We emphasize two specific aspects of shear-induced crystallization in i-PP: (1) the mechanism of nucleation of the β-phase and (2) the reason for the increase in kinetics of crystallization of the unoriented crystals (which was observed in the earlier SAXS study[32] but not explained).

Interpretations of WAXD Results. The nature of the crystalline phase, that is, the precise amount and corresponding form (α and β) of the crystals in i-PP melt after shear, has been determined from in situ, time-resolved WAXD experiments. The strong (110) and (040) reflections of α-crystals are clearly seen in the 2D WAXD patterns obtained immediately after shear (Figure 2). The variation in the azimuthal intensity of these reflections suggests that the α-crystals are oriented in the early stages of crystallization. The degree of orientation, however, decreases with time. Initially, reflections of the β-crystals are not observed in the WAXD patterns (β-crystals do not form immediately after shear). The inception time for appearance of oriented α-crystals in the sheared melt is very rapid (less than 30 s) even at low shear rate of 10 s^{-1} (Figure 3), which is about 2 orders of magnitude faster than that of quiescent crystallization. Subsequently, the (300) reflection of the β-crystals is observed in the WAXD patterns. The inception time for appearance of β-crystals at the shear rate of 10 and 102 s^{-1} are 60 and 45 s, respectively.

Mechanism for Nucleation of β-Phase in Sheared i-PP Melt. In crystallization of i-PP under quiescent conditions, the spherulites consist of only unoriented α-crystals and the amount of β-crystals is negligible or zero. In the sheared i-PP melt (without nucleating agents) both oriented α-crystals and β-crystals are seen. Also, it is seen that the oriented α-crystals form first, immediately after shear, and the β-crystals appear soon afterward. The results clearly indicate that the oriented α-crystals are responsible for the growth of β-crystals, as observed previously by other groups.[23-27] The "surface" of growing, oriented α-crystal assemblies (such as the cylindrites as proposed by Varga et al.[23,24]) forms nucleation sites for the growth of β-crystals (in the form of spherulites). Thus, the amount of the β-crystals is expected to depend on the amount of oriented α-crystals in the melt. This is, in fact, observed in both our SAXS and WAXD studies. From the SAXS experiments, it was determined that the amount of oriented crystal fraction in the polymer melt was much lower at low shear rates than at high shear rates. In addition, the results showed that the amount of oriented crystal fraction was very sensitive at low shear rates and reached a plateau at shear rates above 60 s^{-1}. A very similar trend was observed in the growth of β-phase in i-PP melt under the same shear conditions. The amount of β-phase is lower at low shear rates than at high shear rates; the fraction of the β-crystals in the crystalline phase is only 20% at low shear rate (10 s^{-1}) compared to 65−70% at high shear rates (57 and 102 s^{-1}) (Figure 8). These results also show that the difference in the amount of β-phase between the shear rates of 57 and 102 s^{-1} is very small (can be considered to have reached a plateau at high shear rates). Thus, both SAXS and WAXD results clearly support the conclusion that the surface of the oriented α-crystal assemblies provides nucleation sites for the growth of β-crystals in sheared i-PP melts.

Crystallization Kinetics of the Unoriented Crystals. In the SAXS results, 2 orders of magnitude increase in the kinetics of crystallization of both oriented and unoriented crystals was observed.[32] While the increase in the kinetics of oriented crystals has been attributed to the shear-induced nucleation of the oriented crystals, the reasons for the observed increase in kinetics of the unoriented crystals were not offered in our previous work. We now address this interesting observation with the present WAXD results. The WAXD results clearly show that the β-crystals are primarily unoriented during the major growth process. We would like to note that the WAXD patterns during the initial period of growth of β-crystals show azimuthal variations in the intensity of the (300) reflection (Figure 2), which indicates that the initial β-crystals are oriented. This is, in fact, reasonable since the nucleation sites for the β-crystals are the surface areas of the oriented α-crystal assemblies. The further growth of β-crystals is expected to take place spontaneously without any preferential direction of orientation. This is confirmed by the subsequent WAXD patterns that show strong and uniform intensity of the (300) reflection of the β-crystals. The oriented and unoriented nature of the α- and β-crystals, respectively, is also evident from Figure 10. Figure 10A shows the time evolution 1D profiles of the integrated SAXS intensity of oriented crystals, and unoriented crystals, and total crystalline phase, and Figure 10B shows the growth curves of α- and β-crystals and total crystalline phase from corresponding WAXD results under the same shearing conditions (shear rate = 102 s^{-1}, strain = 1430%, T = 140 °C). Curve c in Figure 10A is the profile for the SAXS intensity of the oriented crystals; curve 3 in Figure 10B shows the growth of the α-crystals from WAXD patterns. There is almost a one-to-one correspondence between the two profiles (SAXS curve c and WAXD curve 3) that confirms that the oriented crystals (SAXS) are α-crystals (WAXD). Comparison of curve b from the SAXS intensity profile of

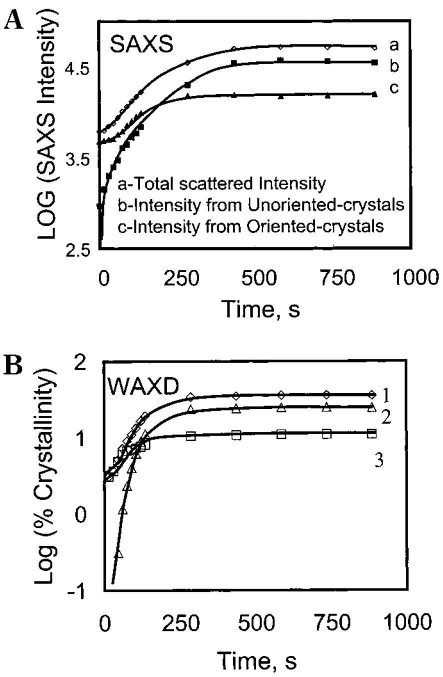

Figure 10. Comparison of growth profiles of integrated scattered intensity from SAXS[31] and of crystalline phase from WAXD (i-PP melt at 140 °C, shear rate = 102 s^{-1}, strain = 1430%): (A) time evolution of the SAXS intensity from the total (a), unoriented (b), and oriented (c) scatterers; (B) time evolution of total crystalline phase (1), β-crystal (2), and α-crystal (3) from WAXD.

the unoriented crystals (Figure 10A) and curve 2, growth of β-crystals from the WAXD profiles (Figure 10B), also shows a remarkable correspondence between the two profiles, which confirms that the β-crystals (WAXD) are the same as the unoriented crystals in SAXS. Note that the half-times of crystallization of the unoriented crystals (SAXS) and the β-crystals (WAXD) as a function of shear rate, illustrated in Figure 9, also show remarkable agreement.

It is interesting to note that the SAXS intensity curve b (of unoriented crystals) shows an increase in intensity immediately after shear as against the time lag observed for the growth of β-crystals (curve 2, Figure 9b). It is conceivable that some of the initially formed α-crystals have low crystalline ordering that are detected by SAXS but not by WAXD. This is particularly evident at low shear rates where the amount of oriented crystals (SAXS) and the amount of β-crystals (WAXD) is low; however, the amount of α-phase is considerably higher, which is due to presence of a large quantity of unoriented α-crystals at lower shear rate conditions.

Conclusions

The WAXD patterns of isotactic polypropylene at 140 °C showed the development of oriented α- crystals immediately (less than 15 s) after application of shear at 1430% strain and shear rates of 10, 57, and 102 s^{-1}. Subsequently (>45 s), growth of β-crystals was observed at all applied conditions of shear.

The amount of β-phase increased with shear rate and reached a plateau value above the shear rate of 60 s^{-1}, which is consistent with SAXS results under the same conditions of applied shear.[31] At a low shear rate of 10 s^{-1}, the β-phase contribution to the total crystalline phase was found to be 20%; it increased to about 65–70% at high shear rates (57 and 102 s^{-1}).

The time lag in the inception of the β-crystals (occurred only after the appearance of oriented α-crystals) and the amount of the induced β-crystals were found to be related to the amount of oriented α-crystals formed under different conditions of shear. This is consistent with the earlier reports that the surface of the oriented α-crystal assemblies (in the form of cylindrites) provides nucleation sites for growth of β-phase in sheared i-PP melts.

WAXD patterns of i-PP after shear showed that the α-crystals were oriented with respect to the shear (or flow) direction and that the β-crystals were unoriented near the end of crystallization. At high shear rates, the trends of the time evolution profiles of the α- and β-crystals agree well with those of the SAXS intensity profiles of the oriented and unoriented scatterers, respectively.

While the increase in the kinetics of crystallization of oriented crystals after shear was observed, as expected, in both SAXS and WAXD experiments, the SAXS experiments showed that the kinetics of crystallization of unoriented scatterers also increase by 2 orders of magnitude. On the basis of comparison of the growth profile of the β-crystals and the SAXS intensity profile of the unoriented scatterers and of the half-time of crystallization of the β-crystals and the unoriented crystals, we attribute the increase of crystallization rate of the unoriented scatterers to the growth of unoriented β-crystals.

Acknowledgment. We record our appreciation to Professor Richard S. Stein for helpful discussions of the subject of flow-induced crystallization. We acknowledge the assistance of Drs. Fengji Yeh, Lizhi Liu, Dufei Fang, and Shaofeng Ran for synchrotron WAXD experimental setup. The financial support for this work was provided by NSF DMR-0098104 and in part by ExxonMobil.

References and Notes

(1) Lee, O.; Kamal, M. R. *Polym. Eng. Sci.* **1999**, *39*, 236.
(2) Pennings, A. J.; Van der mark, J. M. A.; Booij, H. C. *Kolloid Z. Z. Polym.* **1970**, *236*, 99.
(3) Mackley, M. R.; Keller, A. *Polymer* **1973**, *14*, 16.
(4) Pope, D. P.; Keller, A. *Colloid Polym. Sci.* **1978**, *256*, 751.
(5) Miles, M. J.; Keller, A. *Polymer* **1980**, *21*, 1295.
(6) Keller, A.; Kolnaar, H. W. H. *Mater. Sci. Technol.* **1997**, *18*, 189.
(7) Jerschow, P.; Janeschitz-Kriegl, H. *Int. Polym. Process.* **1997**, *12*, 72.
(8) Eder, G.; Janeschitz-Kriegl, H.; Liedauer, S. *Prog. Polym. Sci.* **1990**, *15*, 629.
(9) Eder, G.; Janeschitz-Kriegl, H. *Mater. Sci. Technol.* **1997**, *18*, 268.
(10) Liedauer, S.; Eder, G.; Janeschitz-Kriegl, H. *Int. Polym. Process.* **1995**, *10*, 243.
(11) Liedauer, S.; Jerschow, P.; Geymayer, W.; Ingolic, E. *Int. Polym. Process.* **1993**, *8*, 236.
(12) Kumaraswamy, G.; Issaian, A. M.; Kornfield, J. A. *Macromolecules* **1999**, *32*, 7537.
(13) Kumaraswamy, G.; Varma, R. K.; Issaian; A. M.; Kornfield, J. A.; Yeh, F.; Hsiao, B. S. *Polymer* **2000**, *41*, 8931.
(14) Bayer, R. K.; Eliah, A. E.; Seferis, J. C. *Polym. Eng. Rev.* **1984**, *4*, 201.
(15) Ania, F.; Bayer, R. K.; Tschmel, A.; Michler, H. G.; Naumann, I.; Baltá Calleja, F. J. *J. Mater. Sci.* **1996**, *31*, 4199.
(16) Rueda, D. R.; Ania, F.; Baltá Calleja, F. J. *Polymer* **1997**, *38*, 2027.
(17) Tribout, C.; Monasse, B.; Haudin, *Colloid Polym. Sci.* **1996**, *274*, 197.
(18) Kalay, G.; Bevis, M. J. *J. Polym. Sci., Polym. Phys.* **1997**, *35*, 265.
(19) Huang, H. *J. Appl. Polym. Sci.* **1998**, *67*, 2111.
(20) Wilkinson, A. N.; Ryan, A. J. *Polymer Processing and Structure Development*; Kluwer: Dodrecht, 1998.

(21) Varga, J. *J. Mater. Sci.* **1992**, *27*, 2557.
(22) Huang, M.; Li, X. G.; Fang, B. R. *J. Appl. Polym. Sci.* **1995**, *56*, 1323.
(23) Varga, J.; Karger-Kocsis, J. *J. Polym. Sci., Part B: Polym. Phys.* **1996**, *34*, 657.
(24) Varga, J.; Karger-Kocsis, J. *Polymer* **1995**, *36*, 4877.
(25) Lovinger, A. J.; Chua, J. O.; Gryte, C. C. *J. Polym. Sci., Polym. Phys.* **1977**, *15*, 641.
(26) Lovinger, A. J. *J. Polym. Sci., Polym. Phys.* **1983**, *21*, 97.
(27) Meille, S. V.; Ferro, D. R.; Bruckner, S.; Lovinger, A.; Padden, F. J. *Macromolecules* **1994**, *27*, 2615.
(28) Devaux, E.; Chabert, B. *Polym. Commun.* **1991**, *32*, 464.
(29) Moitzi, J.; Skalicky, P. *Polymer* **1993**, *34*, 3168.
(30) Hubeny, H. D.; Muschik, H. *J. Polym. Sci., Polym. Phys.* **1977**, *15*, 1779.
(31) Nogales, A.; Hsiao, B. S.; Somani, R. H.; Srinivas, S.; Tsou, A.; Balta-Calleja, F. J.; Ezquerra, T. A. *Polymer* **2001**, *42*, 5247.
(32) Somani, R. H.; Hsiao, B. S.; Nogales, A.; Srinivas, S.; Tsou, A.; Sics, I.; Balta-Calleja, F. J.; Ezquerra, T. A. *Macromolecules* **2000**, *33*, 9385.
(33) Dean, D. M.; Rebenfeld, L.; Register, R. A.; Hsiao, B. S. *J. Mater. Sci.* **1998**, *33*, 1.
(34) Dai, P. S.; Cebe, P.; Capel, M.; Alamo, R.; Mandelkern, L. In *Scattering of Polymers*; Cebe, P., Hsiao, B. S., Lohse, D. J., Eds.; ACS Symp. Ser. 739; Oxford: Washington, DC, 2000; p 152.

MA0106191